Three-dimensional Gamut Mapping Method Based on the Concept of Image Dependence

Hung-Shing Chen

Department of Graphic Communications & Technology, Shih Hsin University, Taipei, Taiwan, Republic of China

Hiroaki Kotera▲

Department of Information & Image Science, Chiba University, Chiba, Japan

Three-dimensional (3D) Gamma-Compression Gamut Mapping Algorithm (GMA) is proposed in this study. Currently Gamma-Compression GMA has been designed to work in two-dimensional (2D) Lightness–Chroma planes segmented by primary and secondary hue regions. The advanced 3D GMA is expected to work in 3D uniform color space without color segmentation. This article describes the 3D GMA based on the concept of Image-to-Device (I-D). Considering color gamut relationships between source image and printer device, the Gamma-Compression GMA is applied to the 3D shell shapes in CIE $L^*a^*b^*$ space. 3D gamut shells of a source image and printer device are formed by connecting the surface points located at their gamut surfaces. The surface polygon meshes or parametric cubic surfaces are built up from these most outside color points, and true seamless 3D mapping is performed. It is shown that the GMA coupled with 3D gamut compression and multimapping directions resulted in the better rendition than 2D nonlinear GMAs. It is also shown that 3D Gamma-Compression GMA works better than two known 3D GMAs, CARISMA and minimum ΔE_{94} clipping. Two kinds of focal point decision rules, *Image Lightness Division* (***ILD***) and *Focal Lightness Scaling* (***FLS***), are introduced to find the optimum multimapping directions.

Journal of Imaging Science and Technology 46: 44–52 (2002)

Introduction

In the process of cross-media color reproduction, a key feature is the use of Gamut Mapping Algorithm (GMA) to adjust the different color gamuts between displays and printers. However, most of the current gamut mapping techniques are based on the concept of Device-to-Device (D–D), which is negligent of the image color distributions.

Although the research on 2D GMAs built on Lightness–Chroma planes is active, the ideal GMA is required to work in 3D uniform color space directly. However, few studies about the combination of 3D GMA and image dependence are known. Hence, the development of 3D GMA based on the concept of image dependence is necessary.

When 3D GMA is designed, the following factors should be taken into account.

- 3D description of gamut shell,
- 3D formation of color gamut,
- the type of mapping,
- the mapping direction, and
- the intersection points on gamut surface.

Original manuscript received October 2, 2000

▲ IS&T Member

Color Plates 13 through 21 are printed in the color plate section of this issue, pp. 60–63.

This article represents (1) color gamut description of source image and printing media, (2) 3D gamut shell, (3) the Gamma-Compression GMA,[1] (4) mapping directions toward multifocal points, and (5) the intersection points on the gamut surfaces of source image and printing media.

3D Gamut Mapping Algorithms

Color Gamut Description

Device Gamut. A set of {a*, b*, L*} data is generated with eq.ual intervals of $\Delta a^* = 1$, $\Delta b^* = 1$, $\Delta^* = 5$ in the range of $-120 \le a^* \le 120$, $-120 \le b^* \le 120$, and $0 \le L^* \le 100$ respectively. They can be regarded as monitor initial data with a uniform sampling in CIE L*a*b* space.

Because the distributions of initial data in highlight color are fewer than other areas, more information in monitor highlight area is desirable. The data of $L = 87.5$, $L = 92.5$ and $L = 97.5$ with the interval of $\Delta a^* = 1$, $\Delta b^* = 1$ in the same a^*, b^* ranges is added into the above {a^*, b^*, L^*} initial data.

The corresponding initial RGB data have been limited within the sRGB[2] range and located between 0 and 1. Thus the corresponding {a, b^*, L^*} values filling the sRGB space are used to define sRGB monitor's gamut.

The wireframe gamut of sRGB monitor is shown in **Color Plate 13a, p. 60**. It is formed by extracting the surface points from the generated color distributions. Here, sRGB monitor's color distributions are segmented into m lightness planes and n hue leaves ($m*n$ L–h segments), then color points having the maximum chroma

at each hue leaf represent the gamut surface points. In the example of **Color Plate 13a, p. 60**, 23*36 L–h segments are used to obtain 23*36 surface points. After adding 2 top and bottom points of monitor's color distributions, CRT color gamut will be formed by the $2*m*n$ triangles with these $m*n + 2$ surface points.

On the other hand, the printer gamut is obtained from the measurements of printed color chips. To produce printer color values that are close to a uniform sampling of LAB, the color chips are also formed from the set of {a*, b*, L*} data which is similar to monitor's gamut definition. Therefore, these color chips are printed on superfine paper using an Epson PM-750C inkjet printer.

XYZ tristimulus values of the printed chips are measured with a Gretag spectrophotometer and then transformed into CIE L*a*b* values. As well, the 3D wireframe gamut shape has been formed by segmenting the measured color points into $m*n$ L–h segmented subspaces, and extracting the surface points with the maximum chroma (see **Color Plate 13b, p. 60**)).

Image Gamut. Because image-size is always random, the improved L–h segment technique is applied for describing image gamut.

It is known that the segment-size of color pixels will affect the gamut boundary shape.[3] The larger the segment-size it is, the smoother but less accurate the image gamut boundary it becomes. Therefore, when image gamut is described, the decision of the appropriate segment-size is necessary.

Here, the technique that can remove the surplus pixels but with little effect on gamut shape is introduced into the calculation of image's L–h segments. If $m*n$ L–h segments (m lightness segments and n hue segments) are used to divide i number of image's color distributions, the segment number j in each L–h subspace and the number q of surplus points are calculated as: j is the greatest integer for $j \le i / (m*n)$ and $q = i - m*n*j$. It is thought that the pixels near the image's color centroid can be neglected because they have a week effect on gamut shape. After discarding the 1st *to* q-th surplus points with the minimum distance to the centroid, the image color distributions can be segmented into $m*n$ number of L–h subspaces.

An example of the different image segment-size effect is shown in **Color Plate 14, p. 60**. In a comparison of 3 kinds of image segment-sizes, $10 \times 10/15 \times 15/20 \times 20$ L–h segments, 15×15 L–h segments are selected in this study because this choice appears to offer a better gamut shape than others, having acceptable gamut and more accurate shape.

The $m*n$ number of surface points of source image can be regarded as the color points having the maximum distance to image centroid in each L–h subspace. Then adding two top and bottom points of image's color distributions, image color gamut has been formed according to these $(m*n + 2)$ points. A combined example of test image (15*15 L–h segments) and printer device (23*36 L–h segments) is shown in **Color Plate 15, p. 61**.

3D Gamut Shell

When the surface points of source image and image devices are obtained, their gamut shells can be shaped by the surface modeling technique. In this article, polygon meshes and parametric cubic surfaces are applied to shaping the 3D gamut shell.

The simple way to render color gamut is the formation of the polygon meshes with triangular patches and it has been referred above. However, it is desired that a seamless gamut shell, which is composed of the segmented surfaces can pass through all surface points of the source image or image devices smoothly. A method representing smooth surfaces called *Overhauser Spline Function*[4] is fitted for our cases.

Overhauser Spline Surface $\boldsymbol{P(u,v)}$ based on double parameters u and v on the surface is calculated by Eqs. 1 through 4.

$$P(u,v) = \sum_{i=0}^{3} \sum_{j=0}^{3} N_i^3(u) N_j^3(v) V_{ij}, \quad 0 \le u < 1;\ 0 \le v < 1 \tag{1}$$

$$N_i^3(u) = \left[u^3 u^2 u 1\right] \cdot M_{CR} \tag{2}$$

$$N_j^3(v) = \left[v^3 v^2 v 1\right] \cdot M_{CR} \tag{3}$$

$$M_{CR} = \frac{1}{2} \cdot \begin{bmatrix} -1 & 3 & -3 & 1 \\ 2 & -5 & 4 & -1 \\ -1 & 0 & 1 & 0 \\ 0 & 2 & 0 & 0 \end{bmatrix} \tag{4}$$

where $\boldsymbol{V_{ij}}$ (i = 1,2,3,4 ; j = 1,2,3,4) represents the matrix of 16 control points. Here, the matrix of 16 control points are regarded as a set of 16 segmented surface points described with {a*,b*,L*} data. The first parametric derivative continuity is maintained at nodes where two such Overhauser Spline Surfaces are joined. $\boldsymbol{M_{CR}}$ is called a *Catmull-Rom basic matrix* and it can define the edge located between one segmented surface and its neighboring surface, which contact smoothly.

As shown in **Color Plate 16a, (p. 61)**, a partial *Overhauser Spline Surface* is composed of a set of 16 segmented surface points, and four corners of a partial *Overhauser Spline Surface* segment just pass through four inner surface points. By using this characteristic, the continuous-tone color surface can be formed by Eq. 5 according to the known color values of the four inner surface points (see **Color Plate 16b, (p. 61)**).

$$R(u,v) = (1-u)\,(1-v)\,R_{11} + (1-u)v\,R_{12} + u(1-v)\,R_{21} + uv\,R_{22} \tag{5}$$

where $\boldsymbol{R}(u,v)$ means *Surface Color Function*, and $\boldsymbol{R_{11}}$, $\boldsymbol{R_{12}}$, $\boldsymbol{R_{21}}$, $\boldsymbol{R_{22}}$ represent the color values of 4 inner surface points {$\boldsymbol{V_{11}}$, $\boldsymbol{V_{12}}$, $\boldsymbol{V_{21}}$, $\boldsymbol{V_{22}}$}.

Gamma-Compression GMA

In this study, the basic 2D Gamma-Compression GMA[1] given by Eq. 6 is directly applied to 3D model in CIE L*a*b* space.

$$\overrightarrow{\boldsymbol{pt}} = \overrightarrow{\boldsymbol{po}} \cdot \left(\frac{\overline{\boldsymbol{ps}}}{\overline{\boldsymbol{pi}}} \right)^{\gamma} \tag{6}$$

Here, $\boldsymbol{s}$, $\boldsymbol{t}$, $\boldsymbol{o}$, $\boldsymbol{i}$ and $\boldsymbol{p}$ represent the positions of input color, target color, output gamut, input gamut and the

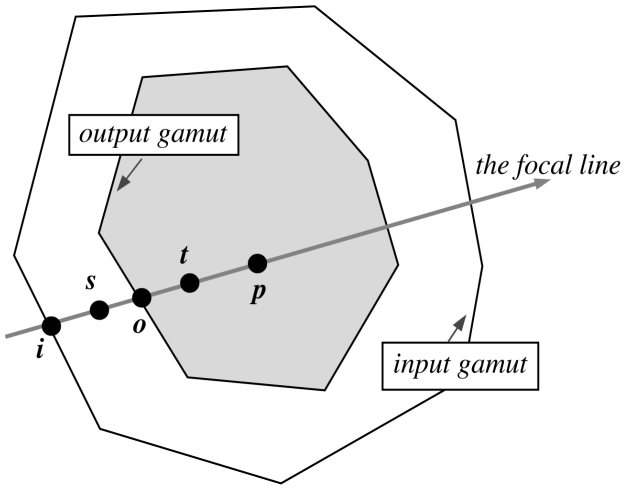

Figure 1. Overview of the relationships between input gamut and output gamut.

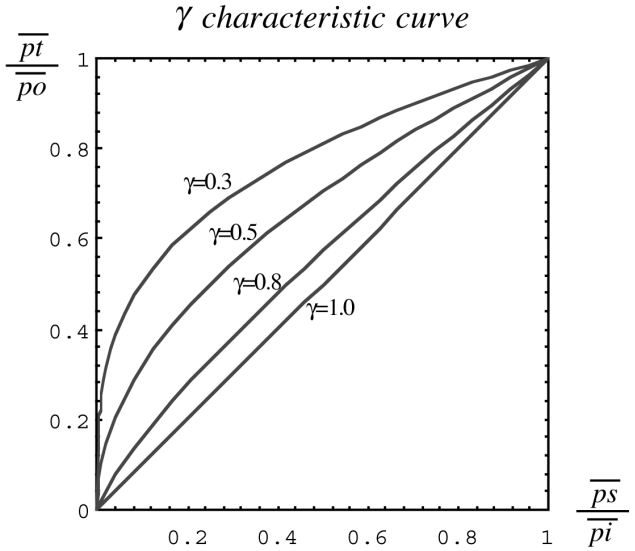

Figure 2. The characteristic curve of Gamma-Compression coefficient γ.

focal point in CIE L*a*b* space respectively (see Fig. 1); γ represents the Gamma-Compression coefficient. The GMA works as linear compression for γ = 1, and as non-linear compression for 0 < γ < 1 (see Fig. 2). The optimum range of γ for 2D Gamma Compression GMA in CIE L*a*b* space was reported to lie around 0.8, and this value is also applicable to 3D Gamma-Compression GMA.

Gamut Mapping Direction

As well known, gamut mapping directions are always dependent on the positions of focal points. In the previous studies of 2D gamut mapping, it has been reported that the method mapped towards multifocal points along curved lines performs superior over the ones mapped towards a single focal point.[5] In this study, two rules called *Image Lightness Division* (***ILD***) and *Focal Lightness Scaling* (***FLS***) are utilized to find the proper positions of focal points in 3D gamut mapping.

An example of image's divided lightness histogram is shown in Fig. 3. To maintain gray balance of the image after mapping, the focal points are selected on L* axis and ***ILD*** is applied to the divided lightness axis of source image. All of image's L* values are segmented into *n* intervals, where each interval includes the same *k* number of samples. Thus *n* number of focal points $\{\boldsymbol{p}_i\}$; i = 1 ~ *n* are decided as the lightness centroid in each L* interval. $\boldsymbol{p}_i$ is calculated as follows.

$$\boldsymbol{p}_i = \frac{\sum_{j=1}^{k} L_{ij} f_{ij}}{\sum_{j=1}^{k} f_{ij}}, \quad i = 1 \sim n \tag{7}$$

where L_{ij} represents the *j-th* lightness value in the *i-th* interval, and f_{ij} represents the occurrence frequency of lightness L_{ij}.

The ***ILD*** rule means that the focal points are decided by slight adaptation of lightness. However, to avoid the chroma ingredients in image's yellow region tending to lower when ***ILD*** method is applied, the first L* value of focal point in highlight range is replaced by the L* value of printer's gamut cusp which is located at the same L* interval.

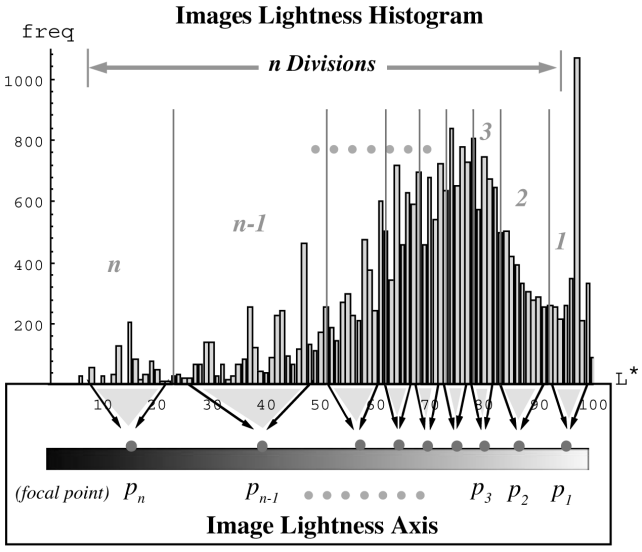

Figure 3. An example of image's divided lightness histogram.

Overview of ***FLS*** rule is shown in Fig. 4. Because it is known that the input image's L* range ($\boldsymbol{J}_{img}$) are wider than the output printer's L* range ($\boldsymbol{J}_{out}$) and the focal range $\boldsymbol{J}_{focal}$ (L* range in which focal points are located) is limited on the printer's L* axis, all positions of focal points can be sought by rescaling $\boldsymbol{J}_{img}$ into $\boldsymbol{J}_{focal}$. In this study, the image pixels in 3D color space are mapped toward their corresponding focal points which are found by linear lightness rescaling equations, Eq.s. 8 and 9.

$$\left(\boldsymbol{J}_{focal}^{up} - \boldsymbol{J}_{focal}^{down}\right) = k \cdot \left(\boldsymbol{J}_{out}^{\max} - \boldsymbol{J}_{out}^{\min}\right), \quad 1 \geq k \geq 0 \tag{8}$$

$$\boldsymbol{J}_{\boldsymbol{focal}} = \boldsymbol{J}_{out}^{down} + \left(\boldsymbol{J}_{\boldsymbol{img}} - \boldsymbol{J}_{in}^{\min}\right) \cdot \frac{\left(\boldsymbol{J}_{focal}^{up} - \boldsymbol{J}_{focal}^{down}\right)}{\left(\boldsymbol{J}_{in}^{\max} - \boldsymbol{J}_{in}^{\min}\right)} \tag{9}$$

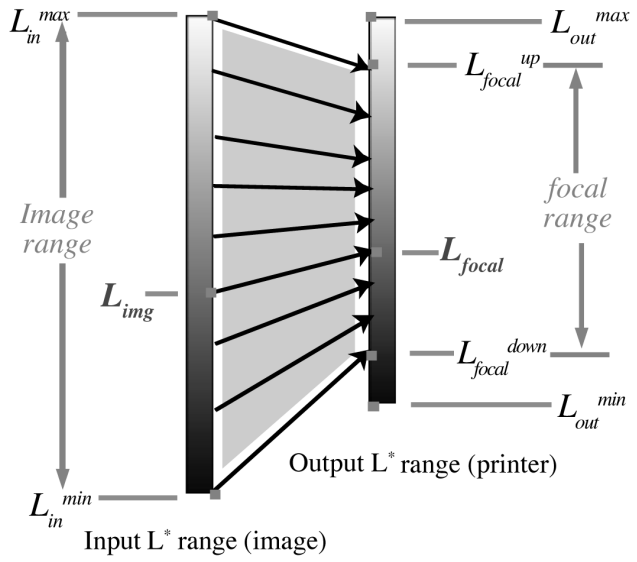

Figure 4. Overview of Focal Lightness Scaling.

where J_{focal} and J_{img} represent the lightness values of focal point and input image color respectively. $J_{in^{max}}$, $J_{in^{min}}$, $J_{out^{max}}$ *and* $J_{out^{min}}$ represent the maximum, minimum values of input, output L* ranges respectively. $J_{focal^{up}}$ *and* $J_{focal^{down}}$ represent the top and bottom L* values of focal range respectively. In Eqs. 8 and 9

$$\left(J_{focal}^{up} - J_{focal}^{down}\right)$$

means the focal range, and in Eq. 9

$$\left(J_{in}^{\max} - J_{in}^{\min}\right)$$

means the input image range. In order to promise that the focal line always passes through inner printer gamut shell and the appropriate solution (intersection point) will be obtained, J_{focal} must be set to smaller than J_{out}.

The parameter k is designed to adjust J_{focal} range and it is set in the range of 0 and 1. If k is set near 1, the mapping effect will tend to maintain most of lightness adaptation. If k is set near 0, the result will tend to map toward a single focal point.

In this study, both $J_{in^{max}}$ and $J_{out^{max}}$ value are calibrated to 100, $J_{out^{up}}$ is set to 95 which corresponds to the higher chroma value of the printer gamut in highlight region, and parameter k is set to 0.8 which means a slight adaptation of lightness.

Intersection Points on Gamut Surface

As described above, for each color gamut of source image and printing media, the gamut surface is composed of $2*m*n$ triangles according to $m*n + 2$ surface points. Here only one reasonable intersection point $\boldsymbol{Q}_1$ is desired on the surface triangle where the focal line passes through.

As shown in Fig. 5, $\boldsymbol{p}$ and $\boldsymbol{s}$ represent the positions of foal point and input color respectively, and $\boldsymbol{Q}_1$, $\boldsymbol{Q}_2$, .. , $\boldsymbol{Q}_n$ represent all of the intersection points. The values of $\boldsymbol{Q}_1$, $\boldsymbol{Q}_2$, .. , $\boldsymbol{Q}_n$ can be found from the common solutions of the focal line $\overleftrightarrow{sp}$ and the plane equation where the surface triangle is located on. When a focal line $\overleftrightarrow{sp}$ passes through the gamut polygon, four kinds of relationships will result. If $\boldsymbol{p}$ is located inside of polygon (see Figs. 5a and 5b) the intersection point $\boldsymbol{Q}_1$ is desired. Otherwise, if $\boldsymbol{p}$ is located outside of polygon (see Figs. 9c and 9d) the intersection point $\boldsymbol{Q}_1$ is desired.

To be more precise, $\boldsymbol{Q}_1$ in Figs. 5a and 5b is satisfied with Eq. 10, and $\boldsymbol{Q}_2$ in Figs. 5c and 5d is satisfied with Eq. 11.

$$\begin{cases} \overrightarrow{\boldsymbol{pQ_1}} \cdot \overrightarrow{\boldsymbol{ps}} > \boldsymbol{o} \\ \left|\overrightarrow{\boldsymbol{pQ_1}}\right| \geq \left|\overrightarrow{\boldsymbol{pQ_1}}\right|, \quad (i = 2, \ldots, n) \end{cases} \tag{10}$$

$$\begin{cases} \overrightarrow{\boldsymbol{pQ_1}} \cdot \overrightarrow{\boldsymbol{ps}} > \boldsymbol{o} \\ \left|\overrightarrow{\boldsymbol{pQ_1}}\right| \leq \left|\overrightarrow{\boldsymbol{pQ_1}}\right|, \quad (i = 2, \ldots, n) \end{cases} \tag{11}$$

The intersection point $\boldsymbol{Q}_1$ represents the position of input gamut $\boldsymbol{i}$ for image gamut or output gamut $\boldsymbol{o}$ for printer gamut.

Experiments

Two gamut mapping experiments are designed in this study.

[Exp 1]: Testing 3D GMAs introduced in this study and the known 2D GMAs.

[Exp 2]: Testing the best GMA in Exp 1 and two known 3D GMAs, including minimum ΔE_{94} clipping[6] and CARISMA..[7]

As shown in Fig. 6, 3D gamut mapping is carried out by the following procedures:

[Steps 1&2] Three kinds of images from CD-ROM are used for testing GMAs. Two are natural images "balloon" and "bride", and the other is CG image "fruits & vegetables" (see **Color Plate 17, (p. 62)**). The quality estimation features of all sub-image for testing GMAs are listed in Table I.

Images (1) "fig", (2) "pomegranate" and (3) "broccoli", are designed for evaluating the image's middle tone. Image (4) "eggplant", is used to judge bluish hue change after mapping. Image (5) "persimmon", is used to judge false contours after mapping. Image (6) "banana", has brilliant green and yellow colors for evaluating image's highlight regions. Image (7) "balloon", is used to evaluate the image's total feature. Image (8) "bride", is used to evaluate the highlight color. In this study, Images (1) through (7) are designed to test the GMAs in Exp 1, and all images of "fruits & vegetables", "balloon" and "bride" are used to test the GMAs in Exp 2.

To perform the calculations of intersection point $\boldsymbol{Q}_1$ on the gamut shell effectively, the simple way to render gamut surface with triangular patches is used, and 3D triangulated gamut polygons of source image and printing media are formed. The image's reference white is regarded as the same setting as sRGB monitor, and printer's reference white must be calibrated to paper white, which is illuminated by CIE Illuminant D_{65}. Then the tops of image and printer gamut are placed at the same position (near the point of {0, 0, 100} in CIE L*a*b* space).

[Step 3] A comparison experiment of the mapping results with multifocal points and with a single focal point

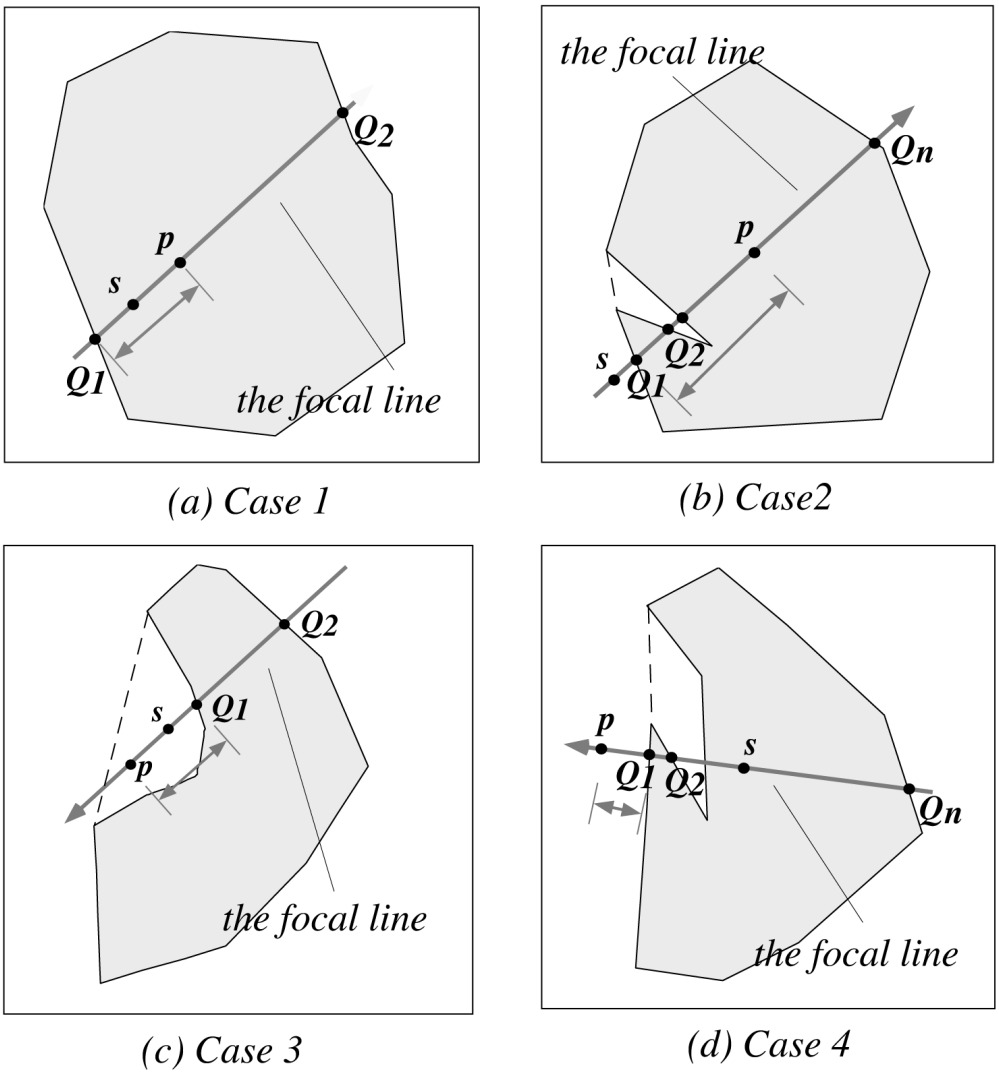

Figure 5. The relationships between the polygon (gamut shell) and the intersection points $\mathbf{Q}_1, \mathbf{Q}_2, \ldots, \mathbf{Q}_n$.

TABLE I. Composition of Test Images.

No.	Subimage name	Color (hue)	Attention point
T1	fig	yellow+red	middle tone
T2	pomegranate	yellow+red	middle tone
T3	broccli	green	middle tone
T4	eggplant	blue+magenta	blue hue loci
T5	persimmon	yellow+red	false contour
T6	banana	yellow	highlight
T7	balloon	all	all

is carried out. For multifocal points, three kinds of lightness divisions by ***FLS*** and ***ILD*** rule (the segmented number $\boldsymbol{n}$ is set to 15, 22 and 30 respectively) are used to decide the mapping directions. For a single focal point, two kinds of the fixed positions (L^* = 75 and 85) on the L^* axis are selected.

[Step 4] By seeking the intersection points on the gamut shell as given above, all positions of input color $\boldsymbol{i}$ and output color $\boldsymbol{o}$ in Eq. 1 are determined. The intersection points $\boldsymbol{Q}_1$ shown in Fig. 5 represent the positions of $\boldsymbol{i}$ for image gamut or $\boldsymbol{o}$ for printer gamut.

[Step 5] For judging input colors locate inside or outside the printer's gamut, $\overline{|ps|}$ (the length of focal point to input color) and $\overline{|po|}$ (the length of focal point to output gamut) are compared. If $\overline{|ps|} > \overline{|po|}$, see Step 6 to perform gamut mapping. If not, jump to Step 7.

[Step 6] All kinds of mapping tests in Exp 1 (see Table II) are performed. By setting the Gamma-Compression coefficient $\gamma = 0.8$, the target colors $\boldsymbol{t}$ in Eq. 6 are calculated. The images mapped by 3D GMAs are also compared with two kinds of 2D GMAs, Image-to-Device Gamma Compression GMA ($\gamma = 0.8$) and Clipping.

After testing the GMAs in Exp 1, the best one is picked to compare with two known 3D GMAs, minimum ΔE_{94} clipping (***Min*** $\Delta \boldsymbol{E_{94}}$ ***Clipping***) and CARISMA based on Device-to-Device (***CARISMA (D-D)***). The features of testing 3D GMAs in Exp 2 are listed in Table III.

[Steps 7&8] In hardcopies, color correction is indispensable to convert RGB data into CMY signals. In this study,

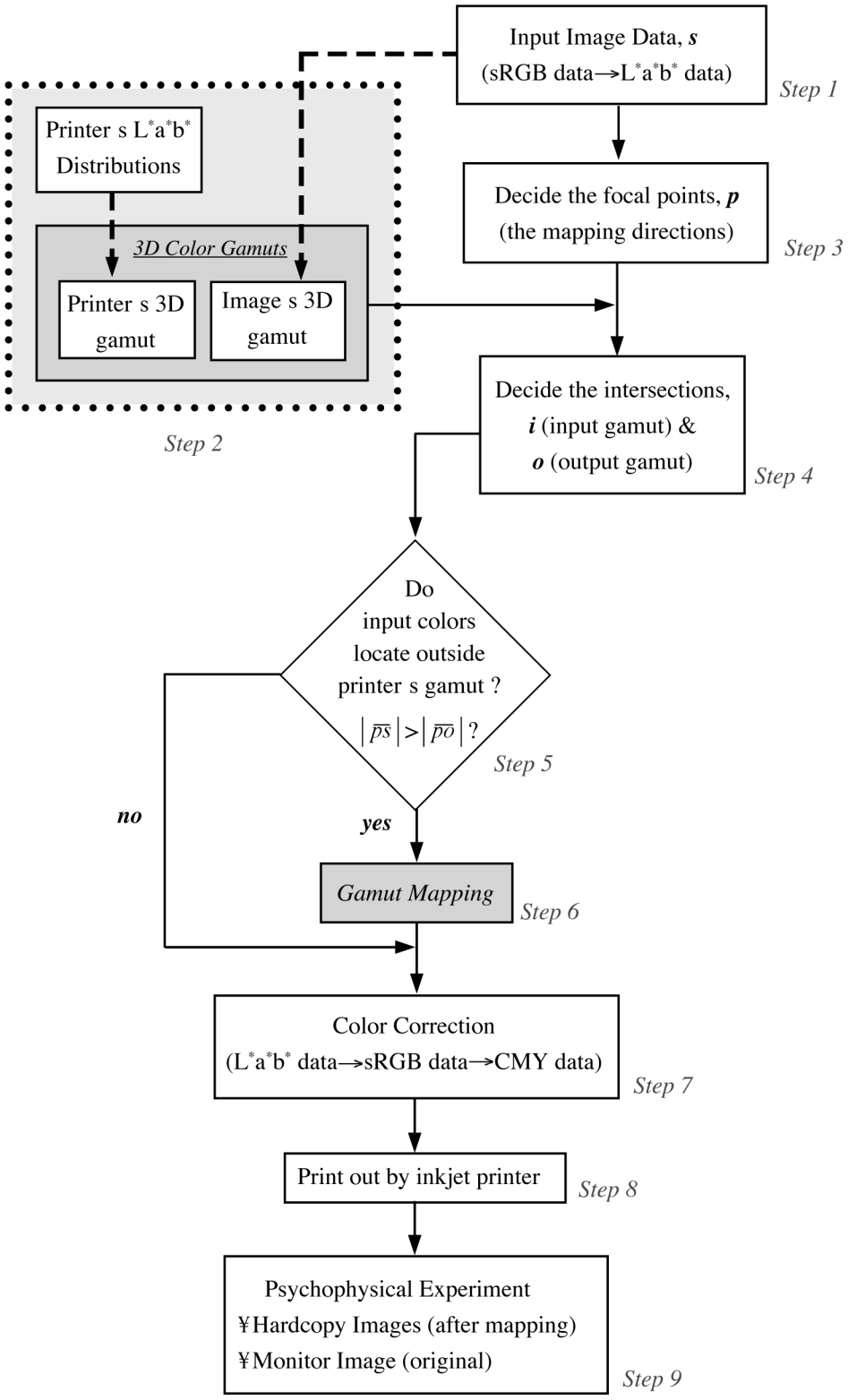

Figure 6. Flow diagram of 3D gamut mapping process.

TABLE II. GMAs Tested in Exp 1.

No.	Notation	Space/Mapping Method	Setting
1	3D_ILD_div15	3D/ILD	Divided numbers = 15
2	3D_ILD_div22	3D/ILD	Divided numbers = 22
3	3D-ILD_div30	3D/ILD	Divided numbers = 30
4	3D-FLS	3D/FLS	linear scaling
5	3D_L75	3D/Fixed focal point	$L^* = 75$
6	3D_L85	3D/Fixed focal point	$L^* = 85$
7	2D_γ 0.8	2D/Image-to-Device	$\gamma = 0.8$
8	2D_cp	2D/Clipping	

TABLE III. 3D GMAs Tested in Exp 2.

Name	3D GMA	Type	Using Gamut Boundary Function	Selection of Focal Point(s)
CARISMA (D-D)	CARISMA	D-D	Monitor & Printer	Multifocal points
Min ΔE_{94} Clipping	Clipping with the miminum ΔE_{94} value	Clipping	Printer	Single focal point

the color correction LUTs embedded in ColorSync® profiles are applied to RGB-CMY conversion. All hardcopies of high quality produced in Exp 1 and Exp 2 are printed out by inkjet printer.

[Step 9] The monitor's white point is set to the chromaticity near CIE Illuminant D_{65} with a peak luminance of 80 cd/m^2. The printed hardcopies after mapping are viewed in a light booth with the same color temperature and peak luminance as the monitor's setting.

A psychophysical experiment has been carried out to make a comparison of color appearance matching between the original CRT image and the printed hardcopies after mapping. A paired-comparison technique[8] is used and both images were appraised by 12 observers in a dim viewing surround where the level of ambient illumination is approximately 64 lux. Using Thurstone's law of comparative judgement,[9] the data from the psychophysical experiment are analyzed to generate interval scales (mean values of z-score values).

Results

An example of color gamuts of test image and image devices formed by *Overhauser Spline Surface* is demonstrated in **Color Plate 18, (p. 62)**. It hints that the smooth gamut surfaces formed by this way can do intersection point calculations more exactly if it is applied into 3D GMAs. Now this algorithm is under development.

An example of out-of-gamut regions of test images for 3D clipping is shown in **Color Plate 19, (p. 62).** These out-of-gamut regions are necessary for gamut compression.

The color distributions of "fruits and vegetables" image mapped by 3D Gamma Compression GMA is shown in **Color Plate 20d through 20 f, (p. 63)**. In comparison with original color distributions in **Color Plate 20a through 20c, (p. 63)**, the image's {a^*, b^*, L^*} distributions after mapping are almost well shifted inside printer gamut.

Figure 7 demonstrates the evaluation result of Exp 1 in the psychophysical experiment. The vertical axis shows the names of eight kinds of GMAs and the horizontal axis represents the interval scale. The title "Total Average" represents the total average value obtained for No. (1) through No. (7) sub-images. "Fruits (5)" represents the interval scale for the persimmon image and "Fruits (6)" represents the score for the banana image. The evaluation result of "Total Average" shows that the 3D GMAs based on multimapping directions resulted in better rendition than the two tested 2D GMAs; 3D mappings using ***ILD*** and ***FLS*** rules with multimapping directions gives better appearance than results mapped toward a single focal point. The groups of ***3D_ILD*** have the first three high rankings and ***3D_ILD_div30*** has the best score. From the evaluation result of "Fruits (5)", 2D Clipping (***2D_Cp***) has the lowest score of all GMAs insofar as it results in unnatural artifacts, i.e., false contours, in the persimmon image. All 3D GMAs work better than 2D GMAs in Exp 1.

According to the evaluation result of "Fruits (6)" in Exp 1, the GMAs mapped toward a single mapping direction, i.e., ***3D_L75*** & ***3D_L85***, are worse, and ***FLS*** and all ***ILD*** rules work well in the banana image. It indicates that the adoption of multimapping directions in 3D mapping can enhance the perception of lightness, particularly in image's yellow highlight regions.

In Exp 2, the best GMA ***3D_ILD_div30*** in Exp 1 is picked up and compared with two kind of 3D GMAs, "***Min ΔE_{94} Clipping***" and "***CARISMA (D-D)***". A mapping example of test image "fruits and vegetables" is shown in **Color Plate 21, (p. 63)**.

The evaluation result of Exp 2 shows that ***3D_ILD_div30*** has the best score, while ***CARISMA (D-D)*** yields a worse result because mapped images lose a little more detail in the rendition of gradation and chroma (see Fig. 8). ***Min ΔE_{94} Clipping*** is better than CARISMA because it retains the color details unmoved inside the printer gamut. The "*persimmon*" image of **Color Plate 21, (p. 63)** shows that ***Min ΔE_{94} Clipping*** adopting a single focal point results in unnatural artifacts in high chroma regions and declination in lightness rendition. In comparison with these two tested 3D GMAs, ***3D_ILD_div30*** using **ILD** rule has the best score.

Conclusions

3D Gamma-Compression GMA based on Image-to-Device is proposed. It is shown that the GMA coupled with 3D

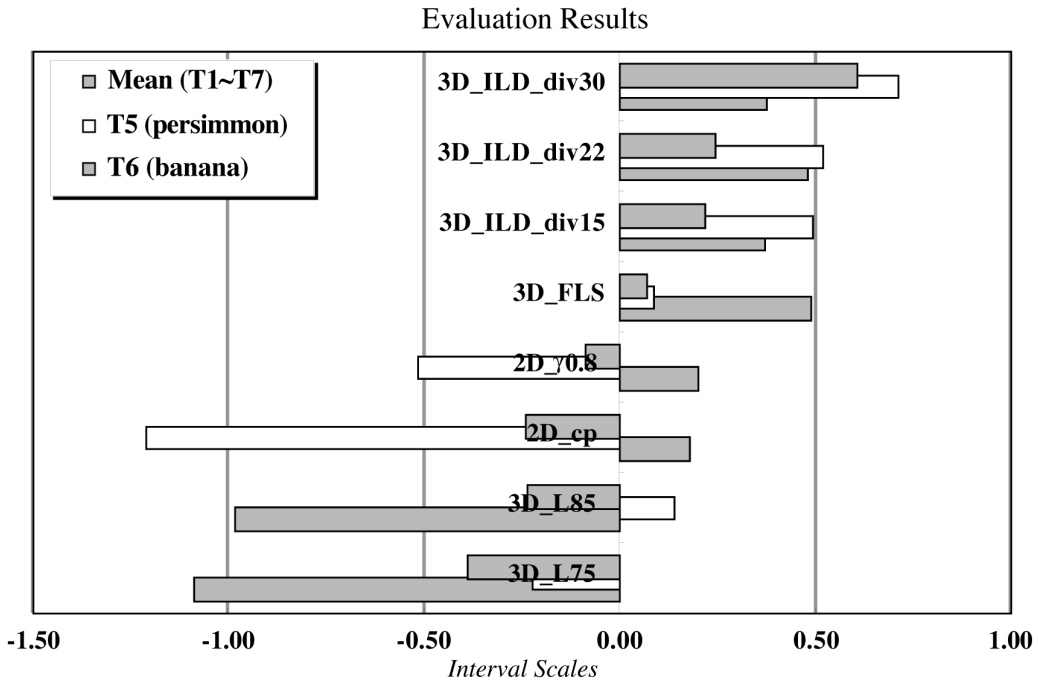

Figure 7. Evaluation result of Exp 1.

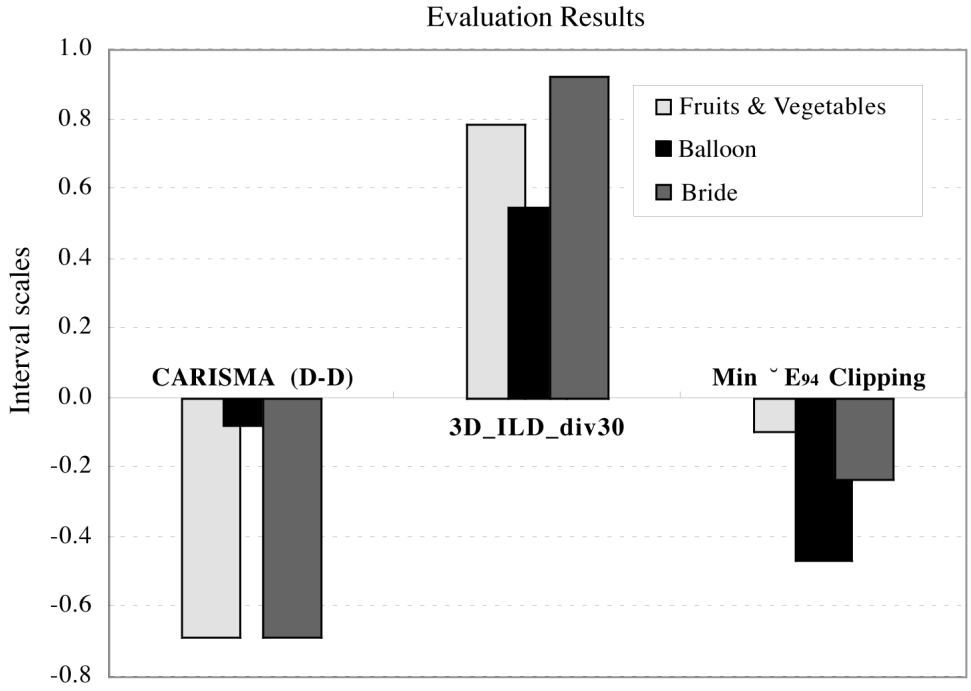

Figure 8. Evaluation result of Exp 2.

gamut compression and multimapping directions, not only resulted in the better rendition than 2D nonlinear Gamma-Compression GMAs, but also works better than two kinds of known 3D GMAs: CARISMA and minimum ΔE_{94} clipping.

It is a key point that a true 3D GMA gives seamless mapping without color segmentation, thus without causing unnatural artifacts as compared with 2D GMA in hue divided L^*–C^* planes, or 3D GMA: CARISMA based on Device-to-Device and minimum ΔE_{94} clipping.

Considering the 3D mapping effects in terms of multi versus single mapping directions, we find that the rule of *Image Lightness Division*, which is dependent on image's lightness distributions, can enhance the perception of lightness and chroma of test images after mapping. It is superior to the GMA mapped toward a single mapping direction.

References

1. H.-S. Chen, M. Omamiuda and H. Kotera, Adaptive Gamut Mapping Method Based on Image-to-Device, *Proc. IS&Ts NIP15*, IS&T, Springfield, VA, 1999, pp. 346–349.
2. *A Standard Default Color Space for the Internet-sRGB*, http://www.w3.org/Graphics/Color/sRGB.
3. J. Morovic and Pei-Li Sun, The Influence of Image Gamuts on Cross-Media Colour Image Reproduction, *Proc. IS&T/SID 8th Color Imaging Conf.*, IS&T, Springfield, VA, 2000, pp. 324–329.
4. J. D. Foley, A. van Dam, S. K. Feiner, and J. F. Hughes, *Computer Graphics: Principles and Practice*, Addison Wesley, Boston, MA, 1996, pp. 504–505.
5. P. G. Herzog and H. Buring, Optimizing Gamut Mapping: Lightness and Hue Adjustments, *Proc. IS&T/SID 7th Color Imaging Conf.*, IS&T, Springfield, VA, 1999, pp. 160–166.
6. N. Katoh, M. Ito and S. Ohno, Three-dimensional gamut mapping using various color difference formulae and color spaces, *J. Electronic Imaging* **8**, 365–379 (1999).
7 J. Morovic, *To develop a universal gamut mapping algorithm*, Ph.D. thesis (1998).
8 L. L. Thurstone, A Law of Comparison Judgement, *Psych. Review* 273–289 (1927).
9 K. M. Braun, M. D. Fairchild and P. J. Alessi, Viewing Techniques for Cross-Media Image Comparisons, *Color Res. Appl.* **21**, 6–17 (1996).